

Spin crossover, structural change, and metallization in NiAs-type FeO at high pressureHaruka Ozawa,^{1,2,*} Kei Hirose,^{1,2} Kenji Ohta,³ Hirofumi Ishii,⁴ Nozomu Hiraoka,⁴ Yasuo Ohishi,⁵ and Yusuke Seto⁶¹*Institute for Research on Earth Evolution, Japan Agency for Marine-Earth Science and Technology, 2-15 Natsushima-cho, Yokosuka, Kanagawa 237-0061, Japan*²*Department of Earth and Planetary Sciences, Tokyo Institute of Technology, 2-12-1 Ookayama, Meguro, Tokyo 152-8551, Japan*³*Center for Quantum Science and Technology under Extreme Conditions, Osaka University, 1-3 Machikaneyama-cho, Toyonaka, Osaka 560-8531, Japan*⁴*National Synchrotron Radiation Research Center, 101 Hsin-Ann Road, Hsinchu Science Park, Hsinchu 30076, Taiwan*⁵*Japan Synchrotron Radiation Research Institute, 1-1-1 Koto, Sayo, Hyogo 679-5198, Japan*⁶*Department of Earth and Planetary Sciences, Kobe University, 1-1 Rokkodai-cho, Nada, Kobe 657-8501, Japan*

(Received 11 July 2011; revised manuscript received 8 September 2011; published 14 October 2011)

We report high-spin to low-spin crossover of iron in NiAs (B8)-type Fe_{0.96}O (FeO hereafter) at high pressure by a combination of *in-situ* x-ray emission spectroscopy (XES) and x-ray diffraction (XRD) measurements. The XES spectra show a loss of spin in B8-type FeO approximately above 119 GPa at 300 K, consistent with the $\sim 2.5\%$ volume reduction around 120 GPa. The high-temperature XRD study also demonstrates a similar volume decrease at 1560–1780 K under the same pressure condition. While the crystal structure of FeO remains to be B8 type across such volume reduction, the atomic arrangements of Fe and O change from inverse to normal NiAs form with considerable decrease in c/a axial ratio. With recent electrical resistance measurements, these suggest that iron spin crossover, inverse-normal structural change, and insulator-metal transition occur concurrently in B8 FeO around 120 GPa.

DOI: [10.1103/PhysRevB.84.134417](https://doi.org/10.1103/PhysRevB.84.134417)

PACS number(s): 75.30.Wx, 91.60.Gf, 91.60.Pn

I. INTRODUCTION

Iron monoxide (FeO) is a fundamental component in the Earth's interior, and therefore its physical properties have been extensively studied at high pressure (P) and temperature (T). Since FeO is one of the archetypal Mott insulators, its high P - T behavior is of great interest also in material sciences and condensed-matter physics. FeO crystallizes in NaCl-type (B1) structure at ambient conditions and undergoes a phase transition into rhombohedrally distorted B1 (rB1) structure above 16 GPa (Fig. 1).¹ Fei and Mao² observed further transition to NiAs-type (B8) structure above 90 GPa at 600 K.

The electronic spin state of iron in FeO has been examined at high pressure but still remains controversial. While high-spin to low-spin crossover was once suggested above 90 GPa based on Mössbauer spectroscopy,³ x-ray emission spectroscopy (XES) measurements performed by Badro *et al.*⁴ demonstrated that high-spin FeO was preserved, at least to 143 GPa at room temperature. More recently Mattila *et al.*⁵ reported that FeO became low-spin state at 140 GPa after laser heating. However, the crystal structure of FeO was determined in none of these earlier studies, and therefore structural control of iron spin state in FeO is not known yet. In addition, the atomic arrangement in NiAs-type FeO has been also a matter of debate. Recent experiments⁶ reported the normal NiAs-type FeO above 140 GPa, while earlier studies showed polytype or inverse NiAs structures below 110 GPa.^{2,7–9} Theory predicted that such atomic arrangement in the NiAs-type structure (inverse or normal) controls the metallicity of FeO.¹⁰

In this paper, we performed a synchrotron XES study to 146 GPa in order to investigate the pressure effect on the spin state of iron in FeO. We also conducted x-ray diffraction (XRD) measurements to identify the crystal structure of FeO and examine the change in volume and atomic arrangement

across the spin crossover. On the basis of recent electrical resistivity measurements⁶ and present structural observations, we also discuss the insulator-metal transition in B8 FeO.

II. EXPERIMENTAL PROCEDURES**A. X-ray emission spectroscopy**

X-ray emission spectroscopy is an established technique widely used to study high-spin to low-spin crossover in transition-metal elements and their compounds (e.g. Refs. 4 and 11). For samples containing iron in a high-spin state, the emission spectra consist of $K\beta_{1,3}$ main peak at 7058 eV and satellite $K\beta'$ peak located at lower energy appearing as a result of the exchange interaction between $3p$ core-hole and $3d$ in a final state of the emission process. The iron spin crossover results in a loss of $3d$ magnetic moment, leading to a disappearance of such satellite peak. High-resolution x-ray emission spectra of the Fe $K\beta$ line were obtained for Fe_{0.96}O at the BL12XU beamline of SPring-8.¹² Such measurements were carried out at room temperature in a diamond-anvil cell (DAC) with decreasing pressure from 34 to 0 GPa (run #1) and from 146 to 103 GPa (run #2). We used flat anvils with 300- μ m culet and beveled anvils with 90- μ m culet in runs #1 and #2, respectively. The starting material was Fe_{0.96}O powder commercially available from Kojundo Chemical Laboratory Co. Ltd., the same as that used previously.¹³ The fine powder of FeO was loaded together with thermal insulation layers of SiO₂ glass into an x-ray translucent gasket that was composed of cubic boron nitride and beryllium. Such a composite gasket can increase the thickness of the sample chamber and reduce the contribution from iron impurity in beryllium. The sample was compressed to high pressure at 300 K and then heated by laser from both sides. The high-pressure phase was subsequently identified by XRD measurement. Pressure was determined at

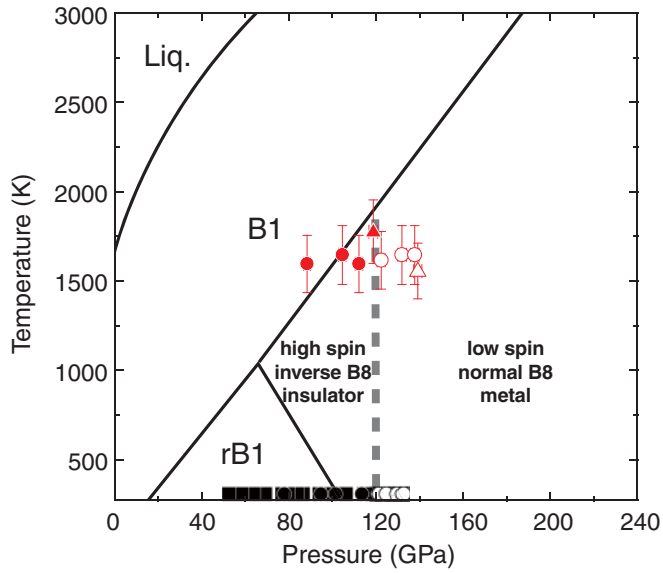


FIG. 1. (Color online) Phase diagram of FeO. Solid lines represent phase boundaries reported by previous studies.^{2,13,25} Solid and open symbols indicate the high-spin/inverse and low-spin/normal B8-type phases, respectively (squares, run #3; circles, run #4; triangles, run #5).

room temperature based on the Raman shift of the T_{2g} mode of the culet of diamond anvil.¹⁴

We used monochromatic x-rays at 11 keV as an incident beam for XES measurements. It was collimated to $\sim 15 \mu\text{m}$ in diameter at the sample. A 1-m Rowland circle type spectrometer, equipped with 1-m spherical bent Ge (620) analyzer, was used to acquire the emission spectra. These spectra were collected through the gasket in order to avoid a loss of intensity due to absorption by the diamond. The spectra covered the energy range from 7020 to 7080 eV with a resolution of 0.8 eV. X-ray diffraction measurements were carried out before or after each XES measurement in order to identify the crystal structure of FeO at high pressure.

B. X-ray diffraction studies

In order to explore the change in volume and atomic arrangement in NiAs-type FeO, we also performed XRD measurements at the BL10XU of SPring-8.¹³ A total of four runs (runs #3–6) were carried out between 52 and 139 GPa in a DAC. The starting material was the same as that used in the present XES measurements. We compacted the sample powder into pellet and then coated the surface of the sample with gold on one side that served as a pressure standard. Only in run #6, gold foil was placed on the FeO sample. It was loaded into a hole in a pre-indented rhenium gasket together with thermal insulation layers of SiO_2 glass. They were compressed by beveled diamond anvils with 120- μm culet. Angle-dispersive XRD patterns were collected on an imaging plate or a charge coupled device. A monochromatic incident x-ray beam with a wavelength of 0.41238–0.42052 Å was collimated to about a 6- μm area (full-width of half maximum) on the sample. Two-dimensional XRD images were integrated as a function of 2θ angle in order to have a conventional one-dimensional diffraction profile using the IPAnalyzer.¹⁵ The samples were

heated to 1560–1780 K by a couple of fiber lasers using the double-sided heating technique. Temperature was measured by fitting the thermal radiation spectrum to the Planck radiation function using the spectroradiometric method.¹⁶ The temperatures below 1400 K were estimated from the relationship between laser output power vs measured sample temperature at >1400 K in run #6.⁶ The radial variations in temperature within an area from which XRD was collected were about $\pm 10\%$.¹³ The sample pressure was calculated from the unit-cell volume of gold using 111 peak, based on the thermal equation of the state of gold proposed by Hirose *et al.*¹⁷ The uncertainty in pressure at high temperature was less than ± 2 GPa, which was derived from the uncertainty in temperature in the application of the thermal equation of state. The unit-cell volume of B8 FeO was obtained from 002, 100, 101, and 102 peaks. We collected the pressure-volume data for B8-type FeO with increasing or decreasing pressure. Except for run #3, the sample was thermally annealed by laser heating to 1560–1780 K after each pressure increment or decrement.

III. RESULTS

A. Spin state of iron

In the first set of experiments, the sample was squeezed to 28 GPa at room temperature. On heating at around 1500 K for 15 min, the pressure rose to 34 GPa. The XRD peaks from the rB1 phase became sharp upon heating, suggesting a release of differential stress in the sample chamber. Subsequently, the spin state of rB1 FeO was examined by XES measurement at room temperature. The spectrum clearly showed the clear Fe $K\beta'$ satellite peak at 7045 eV (Fig. 2), indicating the high-spin

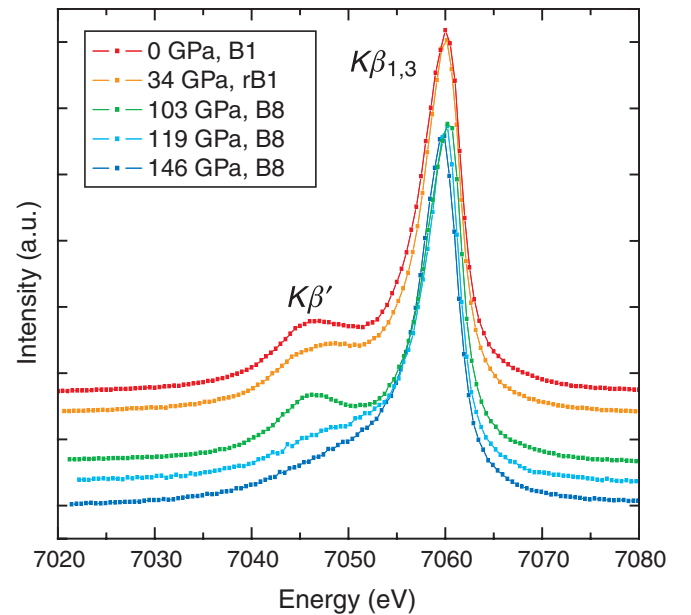


FIG. 2. (Color online) Evolution of x-ray emission spectra of FeO with pressure. All measurements were conducted at room temperature. The spectra are normalized to transmitted intensity and shifted so that the weighted average of main ($K\beta$) plus satellite ($K\beta'$) emission lines is set to 7058 eV. The satellite peak was not observed above 119 GPa, indicating the low-spin state of iron in B8 FeO.

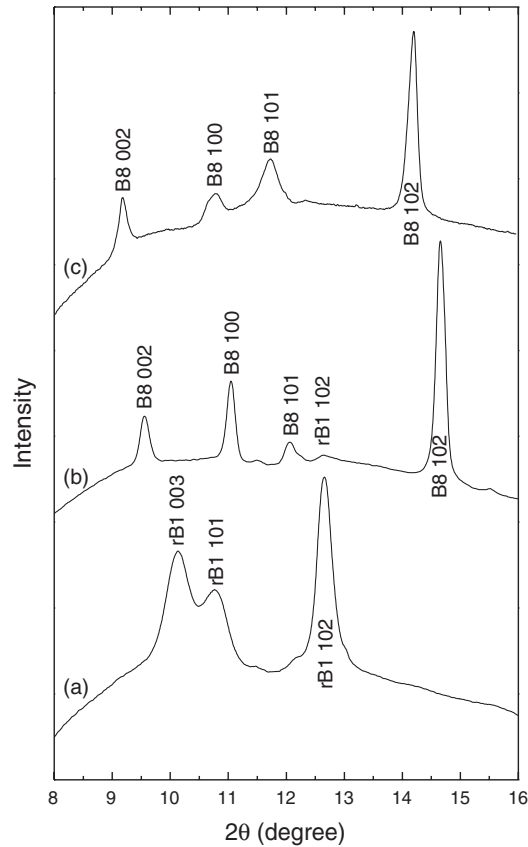


FIG. 3. Room-temperature XRD patterns of FeO collected (a) before and (b) after heating at 146 GPa. (c) Relative peak intensities of B8 FeO changed upon decompression to 103 GPa. All of these patterns were obtained in run #2.

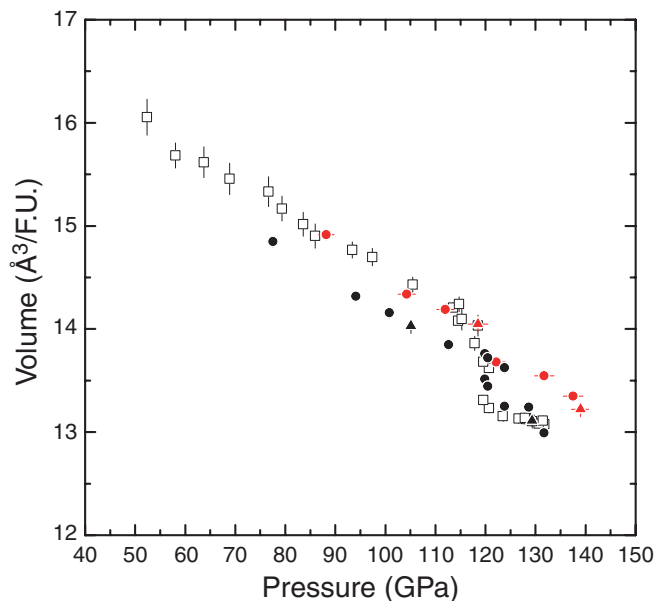


FIG. 4. (Color online) Specific volume of B8 FeO as a function of pressure. Black and red symbols indicate the volumes measured at 300 K and 1560–1780 K, respectively; same symbols as Fig. 1. The data show the abrupt volume change at 120 GPa under both room temperature and high temperature.

state.⁴ Next, we completely released the pressure and obtained the XES spectrum for B1 FeO (Fig. 2).

In the second run, we first compressed the sample to 146 GPa. The broad diffraction peaks from the rB1 phase were observed before heating (Fig. 3). During subsequent heating at 1500–1800 K, the peaks of B8 FeO appeared. After heating for 100 min, almost all the rB1 phase transformed into the B8 phase (Fig. 3). The XES spectrum for such B8-type FeO at 146 GPa revealed the absence of $K\beta'$ satellite peak (Fig. 2), showing the loss of magnetic moment (low-spin state).

Next, we collected the spectra with decreasing pressure down to 103 GPa. A small satellite peak was recognized already at 119 GPa (Fig. 2). The clear $K\beta'$ line was observed at 103 GPa with intensity slightly stronger than that for B1 FeO at 1 bar. Present XRD measurements confirmed the B8-type structure at 103 GPa with no sign of phase transition to a low-pressure phase (Fig. 3), consistent with earlier phase equilibria study.² These indicate the low-spin to high-spin crossover in NiAs-type FeO with decreasing pressure.

B. Volume and structural analyses

We performed additional XRD measurements (runs #3–6) to examine the changes in volume and atomic arrangement in NiAs-type structure. In run #3, the B8 phase was synthesized from rB1 by heating to ~ 2000 K for 60 min at 132 GPa. Then we measured the volume of B8 FeO at room temperature during decompression to 52 GPa without thermal annealing. The obtained pressure-volume data show an abrupt $\sim 5\%$ volume increase at 117–120 GPa (Fig. 4). Next, in runs #4 and #5, the pressure-volume data were collected at both room temperature and high temperature (1560–1780 K). At 300 K, the sudden volume change was again observed at 119–123 GPa, although the jump was about 2.5% (Fig. 4).

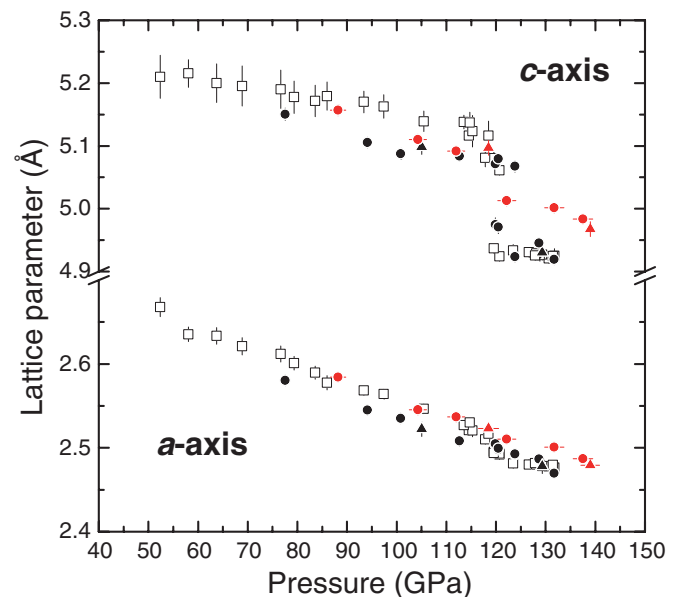


FIG. 5. (Color online) Change in a and c axes of hexagonal B8-type FeO as a function of pressure. Black and red symbols indicate the lattice parameters measured at 300 K and 1560–1780 K, respectively; same symbols as Fig. 1. Only the c axis changes discontinuously at ~ 120 GPa with no anomaly in the a axis.

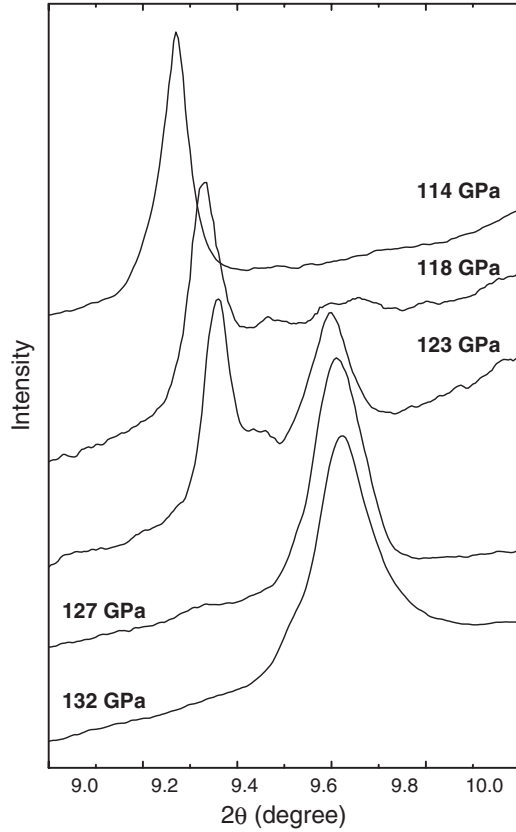


FIG. 6. Change in the 002 peak of NiAs-type FeO with decreasing pressure in run #3. The peaks at $<9.4^\circ$ and $\sim 9.6^\circ$ are from low-pressure (high-spin) and high-pressure (low-spin) B8 phases, respectively.

The larger volume change in run #3 may be attributed to the fact that thermal annealing was not made in this specific run, and therefore the data showed apparently larger volume at a given pressure. At high temperatures of 1560–1780 K, the volume reduction occurred also at 120 GPa with relatively small jump compared to 300 K (Fig. 4), indicating larger thermal expansivity of B8 FeO above 120 GPa.

We notice that such a volume jump in the hexagonal NiAs-type structure is linked to an abrupt increase in the lattice parameter of the c axis (Fig. 5). The 002 peak, which is sensitive to the c parameter, suddenly splits into two peaks upon decompression to 123 GPa, and such peak splitting almost disappears, leaving a single peak at lower angle at 118 GPa (Fig. 6). A similar observation was made for the 102 peak as well. In contrast, no anomaly was observed in the a parameter, indicating a considerable increase only in the Fe-O nearest neighbor distance. Additionally, the relative intensities of 100, 101, and 102 peaks of B8 FeO changed remarkably across such volume increase (Fig. 3), suggesting the modification of atomic arrangement in the NiAs-type structure. The intense 100 and 102 and weak 101 lines of B8 FeO at 146 GPa indicate the normal B8-type structure (Fe in the Ni position in NiAs-type structure), in agreement with the previous studies.^{6,13} On the other hand, the 101 peak grew, and the 100 and 102 lines reduced upon decompression to 103 GPa, indicating a transition to inverse B8 structure (Fe takes the As position in NiAs-type structure) (Fig. 3).

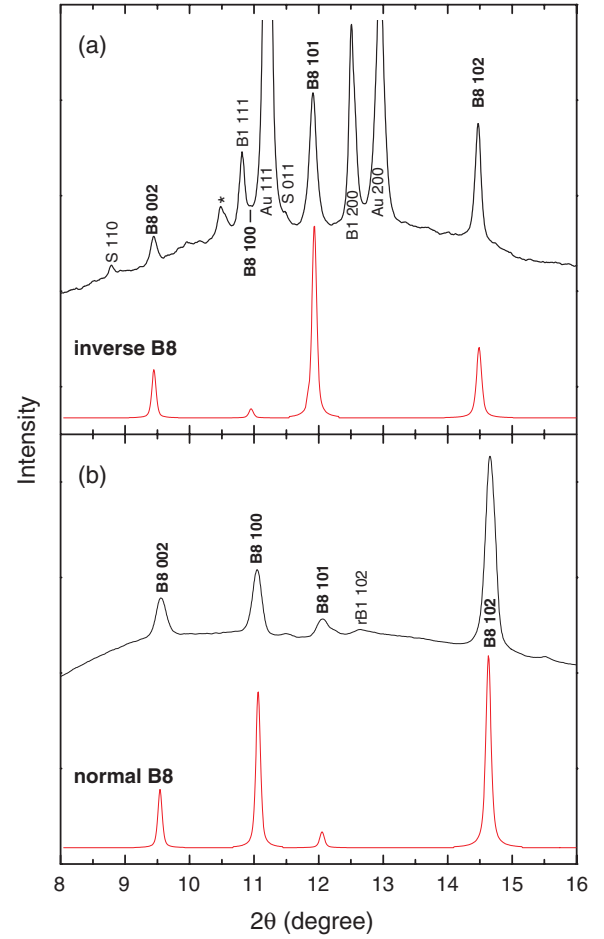


FIG. 7. (Color online) Comparison of observed and calculated XRD patterns for B8 FeO. Black lines show the observed patterns collected at (a) 103 GPa and 1170 K and (b) 146 GPa and 300 K. Red lines demonstrate the calculated patterns for (a) inverse and (b) normal B8 structure. Asterisk in (a) indicates unknown peak. Au, gold; S, CaCl_2 -type SiO_2 (pressure medium).

Run #6 was carried out in order to examine the atomic arrangement in B8 FeO at relatively low pressure. The B8 phase was formed from B1 upon cooling to 1170 K at 103 GPa. The XRD pattern collected from this sample demonstrates the intense 101 peak relative to 100 and 102 lines, clearly indicating the inverse B8 form [Fig. 7(a)].

IV. DISCUSSION

A. Iron spin crossover in B8-type FeO

Present XES measurements indicate a spin crossover of iron from high-spin to low-spin in B8-structured $\text{Fe}_{0.96}\text{O}$ approximately above 119 GPa (minor $K\beta'$ satellite peak was present at 119 GPa, see Fig. 2). The separate XRD measurements revealed the abrupt volume change by 2.5% at 120 GPa and 300 K (Fig. 4), coinciding with the pressure range of the spin crossover found in the XES study. Such a remarkable volume reduction is expected at the iron spin crossover because ionic radius of a transition metal cation is significantly smaller in a low-spin state than in a high-spin state. Anomaly was observed only in the c parameter (Fig. 5),

which is also consistent with the fact that the e_g orbital extending toward surrounding oxygen atoms acquires a couple of electrons upon low- to high-spin crossover, leading to longer Fe-O interatomic distance. Within experimental uncertainty, the anomalous volume jump was observed also at 120 GPa and 1560–1780 K, the same pressure condition as that at 300 K, indicating that the pressure of spin crossover in B8 FeO is not temperature sensitive (Fig. 1). The observed spin crossover pressure is consistent with the prediction by Sherman and Jansen¹⁸ (150 GPa), while Cohen *et al.*¹⁹ proposed much higher crossover pressure (above 500 GPa) for inverse B8 FeO.

The iron spin crossover has been reported to occur in (Mg,Fe)O with B1-type structure around 60 GPa.²⁰ Present volume measurements suggest that the crossover occurs very sharply (Fig. 4), which contrasts with the case of (Mg,Fe)O in which the spin state changes in a wide pressure range, in particular at high temperature.²¹ Recent experimental work by Komabayashi *et al.*²² demonstrated that the high-spin to low-spin crossover occurs in (Mg_{0.81}Fe_{0.19})O between 63 and 96 GPa at 1600–1900 K. Such difference could be due to the negligible Fe-Fe interactions in (Mg,Fe)O when the Fe concentration is small.²¹

B. Normal or inverse NiAs-type structure

In ideal B8-type FeO, Fe occupies either Ni or As position in normal or inverse NiAs-type structure, respectively. One can distinguish between the normal and inverse structures from relative peak intensities.⁸ The calculated XRD patterns of the normal B8 and inverse B8 structures are shown in Fig. 7 with the observed patterns. The XRD pattern collected at 146 GPa shows that low-spin FeO has normal NiAs-type structure [Figs. 3 and 7(b)]. On the other hand, we observed the change in relative peak intensities across the spin crossover in run #3, which suggests a conversion to inverse NiAs-type structure. The conversion was not completed in the present study, possibly due to kinetic hindering of atomic rearrangement at room temperature, whereas the volume changed very sharply. The extensive grain growth occurred at high temperature in runs #4 and #5, which precludes the examination of the change in relative peak intensities. In order to avoid such kinetic hindering of the atomic rearrangement between the normal and inverse structures and the extensive grain growth, we synthesized B8 FeO from the B1 phase by cooling at 103 GPa (run #6). The collected diffraction pattern clearly shows the inverse form [Fig. 7(a)], which further supports the inverse-normal transition across the spin crossover. The inverse NiAs-type structure for high-spin (low-pressure) B8 FeO is also consistent with earlier XRD study below 110 GPa by Kondo *et al.* (Ref. 8).

C. Isostructural insulator, metal transition in B8 FeO

According to theoretical prediction, the normal B8-type FeO is possibly a metal, while the inverse B8 phase is an insulator.¹⁰ Indeed, recent electrical conductivity measurements above 140 GPa revealed that FeO with normal B8 structure is metal, whereas the low-pressure rB1 and B1 phases are semiconductors.⁶ The high-spin B8 FeO below 120 GPa has inverse NiAs-type structure and is thus likely to be insulator, while the low-spin FeO is metal with normal NiAs structure. These characteristics suggest that metallization occurs in B8 FeO concurrently with spin crossover at ~ 120 GPa. This is supported by the temperature-insensitive boundary between the high-spin and low-spin phases (Fig. 1); metallization increases the entropy due to electronic heat capacity, which may cancel the electronic entropy decrease across the high-spin to low-spin crossover. Furthermore, the high-spin B8 phase has smaller thermal expansivity than low-spin B8 (Fig. 4), likely due to its nonmetallic nature. In general, the spin crossover would prevent the onset of metallization because the low-spin Fe²⁺ has completely filled t_{2g} band.²³ In fact, however, the simultaneous pressure-induced magnetic and electronic transition has been reported for Mott insulators such as FeI₂ (Ref. 24) and MnO.¹¹

V. CONCLUSION

We have studied the pressure-induced electronic spin crossover in FeO by a combination of *in-situ* XES and XRD measurements. The XES study showed a loss of magnetic moment in NiAs-type FeO around 120 GPa. We also found $\sim 2.5\%$ volume reduction at 120 GPa and temperatures of both 300 K and 1560–1780 K associated with the change in atomic arrangement from inverse to normal B8 form. Combining with the recent electrical resistance measurements,⁶ iron spin crossover, inverse-normal structural transition, and insulator-metal transition occur concurrently in B8 FeO around 120 GPa.

ACKNOWLEDGMENTS

We are grateful to K. Fujino for his technical support on XES measurements. We also thank T. Komabayashi and R. Wentzcovitch for valuable discussions and comments. The synchrotron XRD experiments were conducted at BL10XU of SPring-8 (Proposal No. 2009B0087, 2010A0087, 2010B0087, and 2011A0087), and the XES experiments were performed at BL12XU with the approval of JASRI/SPring-8 and NSRRC, Taiwan (2009B4264/2010-1-035-1 and 2010A4252/2010-1-035-2). H.O. was partially supported by the Japan Society for the Promotion of Science.

*h-ozawa@jamstec.go.jp

¹T. Yagi, T. Suzuki, and S. Akimoto, *J. Geophys. Res.* **90**, 8784 (1985).

²Y. Fei and H. K. Mao, *Science* **266**, 1678 (1994).

³M. P. Pasternak, R. D. Taylor, R. Jeanloz, X. Li, J. H. Nguyen, and C. A. McCammon, *Phys. Rev. Lett.* **79**, 5046 (1997).

⁴J. Badro, V. V. Struzhkin, J. Shu, R. J. Hemley, H. K. Mao, C. C. Kao, J. P. Rueff, and G. Shen, *Phys. Rev. Lett.* **83**, 4101 (1999).

⁵A. Mattila, J. P. Rueff, J. Badro, G. Vankó, and A. Shukla, *Phys. Rev. Lett.* **98**, 196404 (2007).

⁶K. Ohta, K. Hirose, K. Shimizu, and Y. Ohishi, *Phys. Rev. B* **82**, 174120 (2010).

- ⁷I. I. Mazin, Y. Fei, R. Downs, and R. Cohen, *Am. Miner.* **83**, 451 (1998).
- ⁸T. Kondo, E. Ohtani, N. Hirao, T. Yagi, and T. Kikegawa, *Phys. Earth Planet. Inter.* **143-144**, 201 (2004).
- ⁹M. Murakami, K. Hirose, S. Ono, T. Tsuchiya, M. Isshiki, and T. Watanuki, *Phys. Earth Planet. Inter.* **146**, 273 (2004).
- ¹⁰Z. Fang, I. V. Solovyev, H. Sawada, and K. Terakura, *Phys. Rev. B* **59**, 762 (1999).
- ¹¹C. S. Yoo, B. Maddox, J. H. P. Klepeis, V. Iota, W. Evans, A. McMahan, M. Y. Hu, P. Chow, M. Somayazulu, D. Häusermann, R. T. Scalettar, and W. E. Pickett, *Phys. Rev. Lett.* **94**, 115502 (2005).
- ¹²R. Nomura, H. Ozawa, S. Tateno, K. Hirose, J. Hernlund, S. Muto, H. Ishii, and N. Hiraoka, *Nature* **473**, 199 (2011).
- ¹³H. Ozawa, K. Hirose, S. Tateno, N. Sata, and Y. Ohishi, *Phys. Earth Planet. Inter.* **179**, 157 (2010).
- ¹⁴Y. Akahama and H. Kawamura, *J. Appl. Phys.* **96**, 3748 (2004).
- ¹⁵Y. Seto, D. Nishio-Hamane, T. Nagai, and N. Sata, *Rev. High Pressure Sci. Technol.* **20**, 269 (2010).
- ¹⁶Y. Ohishi, N. Hirao, N. Sata, K. Hirose, and M. Takata, *High Pres. Res.* **28**, 163 (2008).
- ¹⁷K. Hirose, N. Sata, T. Komabayashi, and Y. Ohishi, *Phys. Earth Planet. Inter.* **167**, 149 (2004).
- ¹⁸D. M. Sherman and H. J. F. Jansen, *Geophys. Res. Lett.* **22**, 1001 (1995).
- ¹⁹R. E. Cohen, I. I. Mazin, and D. G. Isaak, *Science* **275**, 654 (1997).
- ²⁰J. Badro, G. Fiquet, F. Guyot, J. P. Rueff, V. V. Struzhkin, G. Vankó, and G. Monaco, *Science* **300**, 789 (2003).
- ²¹T. Tsuchiya, R. M. Wentzcovitch, C. R. S. da Silva, and S. de Gironcoli, *Phys. Rev. Lett.* **96**, 198501 (2006).
- ²²T. Komabayashi, K. Hirose, Y. Nagaya, E. Sugimura, and Y. Ohishi, *Earth Planet. Sci. Lett.* **297**, 691 (2010).
- ²³D. M. Sherman, *Adv. Phys. Geochem.* **7**, 113 (1988).
- ²⁴M. P. Pasternak, W. M. Xu, G. Kh. Rozenberg, R. D. Taylor, G. R. Hearne, and E. Sterer, *Phys. Rev. B* **65**, 035106 (2001).
- ²⁵R. Boehler, *Earth Planet. Sci. Lett.* **111**, 217 (1992).